Title

Synthesis and evaluation of a nanoglobular dendrimer 5-aminosalicylic Acid conjugate with a hydrolyzable schiff base spacer for treating retinal degeneration.



Journal

ACS Nano, 8(1)

Authors

Wu, Xueming
Yu, Guanping
Luo, Chengcai
et al.

Publication Date

2014-01-28

DOI

10.1021/nn4054107

Peer reviewed

Published in final edited form as:
*ACS Nano*. 2014 January 28; 8(1): 153–161. doi:10.1021/nn4054107.

# Synthesis and evaluation of a nanoglobular dendrimer 5-aminosalicylic acid conjugate with a hydrolyzable Schiff base spacer for treating retinal degeneration

**Xueming Wu**[1,5], **Guanping Yu**[1,5], **Chengcai Luo**[2,5], **Akiko Maeda**[3,4], **Ning Zhang**[3], **Da Sun**[1], **Zhuxian Zhou**[1], **Anthony Puntel**[1], **Krzysztof Palczewski**[3], and **Zheng-Rong Lu**[1]

[1]Department of Biomedical Engineering, School of Engineering, Case Western Reserve University, Cleveland, Ohio, USA

[2]Ningbo Institute of Technology, Zhejiang University, Ningbo, Zhejiang, China

[3]Department of Pharmacology, School of Medicine, Case Western Reserve University, Cleveland, Ohio, USA

[4]Department of Ophthalmology, School of Medicine, Case Western Reserve University, Cleveland, Ohio, USA

## Abstract

Biocompatible dendrimers with well-defined nanosizes are increasingly being used as carriers for drug delivery. 5-Aminosalicylic acid (5-ASA) is an FDA approved therapeutic agent recently found effective in treating retinal degeneration of animal models. Here, a water-soluble dendrimer conjugate of 5-ASA (AGFB-ASA) was designed to treat such retinal degeneration. The drug was conjugated to a generation 2 ($G_2$) lysine dendrimer with a silsesquioxane core (nanoglobule) by using a hydrolysable Schiff base spacer. Incubation of nanoglobular $G_2$ dendrimer conjugates containing a 4-formylbenzoate (FB) Schiff base spacer in pH 7.4 phosphate buffers at 37 °C gradually released 5-ASA. Drug release from the dendrimer conjugate was significantly slower than from the low molecular weight free Schiff base of 5-ASA (FB-ASA). 5-ASA release from the dendrimer conjugate was dependent on steric hindrance around the spacer. After intraperitoneal injection, the nanoglobular 5-ASA conjugate provided more effective 7-day protection against light-induced retinal degeneration at a reduced dose than free 5-ASA in *Abca4*$^{-/-}$*Rdh8*$^{-/-}$ mice. The dendrimer 5-ASA conjugate with a degradable spacer could be a good candidate for controlled delivery of 5-ASA to the eye for treatment of retinal degeneration.

### Keywords

dendrimer; 5-aminosalicylic acid; Schiff base; drug delivery; controlled release

It is well known that the aldehyde, all-*trans*-retinal (atRAL) is a major intermediate in the visual cycle.[1–5] Photoactivated rhodopsin releases atRAL, which is subsequently transported

Correspondence to: Dr. Zheng-Rong Lu, Department of Biomedical Engineering, Wickenden Building, Room 427, Case Western Reserve University, 10900 Euclid Avenue, Cleveland, OH 44106-7207, zxl125@case.edu.
[5]Contributed equally to this research

by an ATP-binding cassette transporter 4 (*Abca4*) and reduced to all-*trans*-retinol by all-*trans*-retinol dehydrogenases located in photoreceptor cells. Continuous regeneration of the 11-*cis* chromophore from atRAL is essential for both renewal of light-sensitive visual pigments required for vision and photoreceptor survival in the vertebrate retina.[5] Disruptions in the conversion or clearance of atRAL in photoreceptors can cause accumulation of this reactive atRAL aldehyde and its toxic condensation products with eventual manifestations of retinal dystrophy, including human retinal degenerative diseases such as Stargardt's disease and age-related macular degeneration. Thus, it appears that accumulation of atRAL is one of the key factors initiating retinal photodamage characterized by progressive retinal cell death evoked by both acute and chronic light exposure.

One of the pharmacological innovations to protect against photodamage mediated by atRAL is the use of aldehyde-reactive amines to reversibly sequester atRAL as a Schiff base thereby lowering its tissue concentration.[4] Slow release of atRAL from the Schiff base allows the retinoid to flow back into the retinoid cycle without affecting visual chromophore regeneration and phototransduction.[1,5] As a FDA-approved compound, 5-aminosalicylic acid (5-ASA) containing a primary amine group has a high potential for preventing light-induced retinopathy in a mouse model of human retinal diseases, the *Abca4/Rdh8* (*Abca4*$^{-/-}$*Rdh8*$^{-/-}$) double knockout mouse.[5] However, free 5-ASA exhibits rapid pharmacokinetics ($t_{1/2}$ = 0.4 to 2.4 h)[6] with poor tissue delivery and therapeutic efficacy due to its low water solubility (< 0.9 mg/mL). The use of a suitable drug delivery system can provide better and prolonged therapeutic efficacy at reduced doses. Thus we aimed to design and develop an effective delivery system for sustained delivery of 5-ASA to the retina.

Intraocular drug delivery has been a major challenge due to the unique anatomy and physiology of the eye.[7–10] Due to blood/ocular barriers, conventional drug delivery systems, including solutions, suspensions and gels can only deliver a small percentage of administrated drugs across the cornea, conjunctiva, and sclera to reach affected sites of the retina, especially the posterior segments. As a result, relatively large doses of drugs must be frequently administrated to achieve and maintain therapeutic concentrations in the eyes. Rapid development of biomaterials and increasing understanding of ocular drug absorption and disposition mechanisms have created new possibilities for ocular drug delivery.[11,12] Various new drug delivery systems, including dendrimers, micro-emulsions, mucoadhesive polymers, hydrogels, iontophoresis, microneedles and prodrugs, have been employed to improve the pharmacokinetics and pharmacodynamics of ocular therapeutics.[13–20] These novel delivery systems offer many advantages over conventional formulations due to their improved drug delivery profiles and reduced drug toxicity. Among such advanced delivery systems, polymer-based nanocarriers appear highly attractive and are being extensively investigated.[21,22] Compared with linear polymers, dendrimers are well-defined, globular highly-branched macromolecules with a large number of functional groups at their surface. Moreover, their size, molecular weight, and surface properties can be easily controlled. Dendrimers have attracted much attention in drug delivery due to these unique structural properties and good water solubility.[23–30] Thus a relatively large number of drug molecules can be conjugated to dendrimers with proper chemical spacers to achieve controlled and sustained drug release.

Here we designed and synthesized a G2 nanoglobular conjugate of 5-ASA with a degradable spacer. Nanoglobules are a new class of lysine dendrimers with a silsesquioxane core.[31,32] The G2 nanoglobule has 32 surface amino groups for drug conjugation. A Schiff base spacer is designed to release the drug *via* hydrolysis under physiological condition.[33,34] Drug release from the conjugate was investigated *in vitro* and was compared with that of the free Schiff base of 5-ASA. Finally, the therapeutic efficacy of the conjugate was preliminarily tested in the *Abca4*$^{-/-}$*Rdh8*$^{-/-}$ mouse[4] model *in vivo*.

## RESULTS

### Synthesis of the dendrimer conjugate, AGFB-ASA

The G2 lysine dendrimer with an octa(3-aminopropyl)silsesquioxane (nanoglobule) was synthesized through a divergent approach by reacting octa(3-aminopropyl)silsesquioxane or a lower generation dendrimer with $(Boc)_2$-L-lysine- OH pentafluorophenol active ester in the presence of diisopropylethylamine (DIPEA). The G2 nanoglobule was obtained in 98.0 % yield and high purity. The structure of the G2 nanoglobular dendrimer is shown in Fig. 1a. Standard liquid phase synthesis was used to synthesize the G2 nanoglobular 5-ASA Schiff base conjugate, AGFB-ASA, and the scheme of this synthesis is shown in Fig. 1b. All intermediates and the final product were confirmed by MALDI-TOF mass spectrometry and $^1$H-NMR spectroscopy. The MALDI-TOF mass spectrum and proton NMR spectrum of the final product AGFB-ASA is shown in Figures 2b and 2c. The chemical shift at 0.63 was derived from the 8-methylene proton, and its integral value was assigned as 16. The integral value of the imine proton at chemical shift 8.63 was 5.6 whereas that of the benzene proton on the linker and 5-ASA at the chemical shift from 7.93 to 8.07 was 35.3. Integral values of specific group protons confirmed the assignment of a 1:5:5 composition of the dendrimer:spacer:5-ASA with approximately 5 drug molecules on each G2 dendrimer molecule. The number of attached 5-ASA molecules was also determined by measuring the absorbance of the Schiff base (imine aromatic moiety) in DMSO by UV spectroscopy at 325 nm. The calculated number of 5-ASA residues in the dendrimer conjugate estimated by UV spectroscopy was 5.8, similar to the number (ca. 5) determined by proton NMR spectroscopy. The dendrimer drug conjugate had good water solubility. The free Schiff base conjugate of 5-ASA with 4-formylbenzoic acid was also synthesized and used as a control, Fig. 1d.

### Drug release studies

The release of 5-ASA from the dendrimer conjugate AGFB-ASA was evaluated in phosphate buffers at pH 7.4 and 37 °C along with FB-ASA as a control. Fig. 3 shows the time course of UV spectral change from the conjugates incubated in phosphate buffer. The maximum UV absorption of the Schiff base in PBS was at 325 nm at pH 7.4. Degradation of the Schiff base spacer was reflected by the decrease of absorption at 325 nm over time. Schiff base degradation of AGFB-ASA was much slower than that of the free Schiff base conjugate FB-ASA at pH 7.4. Drug release from both conjugates was calculated from their UV absorption at 325 nm as depicted in Fig. 4a. At physiological pH 7.4, the dendrimer conjugate AGFB-ASA also showed a more controllable release pattern compared to the free Schiff base FB-ASA with the identity of the released drug further confirmed by HPLC (Fig.

4b). The HPLC elution times for 5-ASA released from AGFB-ASA and FB-ASA were 3.335 min and 3.276 min, respectively, consistent with the retention time of the 5-ASA standard (3.331 min).

### Effects of AGFB-ASA on preventing light-induced retinal degeneration

The therapeutic efficacy of the AGFB-ASA conjugate was investigated in 4-week-old *Abca4*$^{-/-}$*Rdh8*$^{-/-}$ mice, after acute strong light exposure. In this animal model of Stargardt's disease, strong light exposure results in accumulation of atRAL which can cause retinal degeneration. The AGFB-ASA conjugate after intraperitoneal administration should release free 5-ASA and reduce the accumulation of atRAL in the retina, preventing light induced retinal degeneration. Schematic representation of the experimental design is presented in Fig. 5a.

Electroretinograms (ERGs) were recorded to evaluate retinal functions after drug pretreatment with either free 5-ASA or conjugate AGFB-ASA at an equivalent dose of 0.5 mg 5-ASA per mouse and subsequent light illumination of *Abca4*$^{-/-}$*Rdh8*$^{-/-}$ mice at 4 weeks age. ERG responses of conjugate AGFB-ASA pretreated light-illuminated mice (AGFB-ASA-LI) were maintained as the no light-illuminated mice (NLI), in contrast to 5-ASA-pretreated light-illuminated mice (free 5-ASA-LI) displayed reduced ERG peak amplitudes ($P < 0.05$, Student's T-test) (Fig. 5b).

Quantitative morphometry of ONL thickness measured by OCT imaging was examined in mice treated with 5-ASA and the conjugate at doses equivalent to 0.5 and 1.0 mg 5-ASA per mouse. AGFB-ASA pretreated light-illuminated *Abca4*$^{-/-}$*Rdh8*$^{-/-}$ mice evidenced a more preserved ONL thickness than free 5-ASA pretreated light-illuminated mice which failed to exhibit any protection against light induced retinal degeneration at 0.5 mg 5-ASA per mouse (Fig. 5c). Of note, drug treatments with the 1.0 mg dose in both formulations prevented retinal degeneration with greater protection conferred by the AGFB-ASA (Fig. 5d). Representative OCT images from light-illuminated 4-week-old mice pretreated with conjugate free 5-ASA or AGFB-ASA are shown in Fig. 5e. AGFB-ASA provided more effective protection against light induced retinal degeneration at the reduced dose than the free drug.

## DISCUSSION

The G2 nanoglobule was synthesized by a modified synthetic method that employed a pentafluorophenol-activated ester of Boc-protected lysine. This modified approach simplified the purification steps, reduced the reaction time and produced nanoglobules with a high yield compared to the previously reported synthetic procedure.[31,32] Immediately after conjugation of the spacer 4-formylbenzoic group to the G2 nanoglobule, the remaining amino groups were blocked by acetylation to neutralize the G2 positive charges. We also tested the effect of differing degrees of drug conjugation on the solubility of the resulting drug conjugates in PBS. The solubility of the nanoglobular 5-ASA conjugate AGFB-ASA decreased significantly when the stoichiometry reached 8 drug molecules per nanoglobule. We found that the conjugate with approximately five 5-ASAs per nanoglobule had good aqueous solubility and carried a reasonable drug load.

It was observed that laser energy of MALDI-TOF mass spectrometry had a significant effect on the analysis of the nanoglobular drug conjugate. With relatively high laser energy, the measured mass value (m/z = 5866.58) was smaller than the calculated value based on the drug content determined by proton NMR and UV spectrometry. But with relatively low laser energy, the MALDI-TOF mass spectrum of the conjugate showed a mass close to the calculated mass (Fig. 2b). Since Schiff bases are not very stable and acid was used as a matrix, the laser with high energy could have broken the imine bond, resulting in a mass lower than the calculated mass for the conjugate. However, with proper laser energy used for MALDI-TOF mass spectroscopy, similar drug loading results were obtained with three different analytical methods, 5.6 drug molecules per nanoglobule on average from $^{1}$H NMR, 5.8 from UV spectroscopy and 5 from mass spectrometry. The size of nanoglobule G2 determined by dynamic light scattering is about 5 nm as reported in a previous publication[35].

Compared to the free Schiff base FB-ASA, AGFB-ASA also had a controllable release profile. This probably was due to steric hindrance around the Schiff base in the nanoglobular conjugate. Although drug release from AGFB-ASA was more controllable than that from the free Schiff base, the overall release rate from AGFB-ASA was still relatively high in aqueous solution. The Schiff base linkage structure could be modified to decrease the hydrolysis rate further and achieve an even more controllable drug release. One possible approach could be to use a ketone group to form a Schiff base with the drug; a steric effect could decrease the hydrolysis rate of this linkage. Another idea would be to introduce an electron-withdrawing group on the benzene ring of 4-formylbenzoic acid to stabilize the Schiff base and decrease the hydrolysis rate. A more controllable and sustained drug release profile would maintain stable drug concentrations *in vivo* and confer more prolonged protective effects on the retina.

To effectively demonstrate the prolonged protective effect of the nanoglobular drug conjugate, we modified the treatment protocol in this study. The *in vivo* circulation half-life of free 5-ASA was noted to be about 2.4 h.[6] In the previous study,[5] free 5-ASA was administrated by oral gavage (2 mg/mouse) 2 h before light exposure, conferring good protection against light-induced retinal degeneration in *Abca4*$^{-/-}$*Rdh8*$^{-/-}$ mice. Here, free 5-ASA or the AGFB-ASA conjugate was intraperitoneally injected at a dose equivalent to 0.5 mg or 1.0 mg 5-ASA per mouse 6 h before light exposure to evaluate the 7 day protective effect of the drug conjugate. Our results showed that the nanoglobular drug conjugate had a greater 7 day effect than free 5-ASA at a reduced dose (0.5 mg/per mouse) in protecting the retinas of 4-week-old *Abca4*$^{-/-}$*Rdh8*$^{-/-}$ mice against bright light-induced retinal degeneration. This observation indicates that the nanoglobular drug conjugate exhibited more prolonged protection against retinal degeneration at a reduced dose due to its controlled and sustained release of 5-ASA. In contrast, the free drug at the low dose was probably cleared from the body much more rapidly, resulting in a diminished retinal protective effect seven days after bright light exposure. A more prolonged protective effect could be achieved by chemical modification of nanoglobular conjugates to achieve a more controllable and sustained drug release profile. Currently, we are focusing on structural optimization of nanoglobular drug conjugates to achieve this goal.

## CONCLUSION

A water-soluble G2 nanoglobular conjugate AGFB-ASA containing a hydrolyzable Schiff base linkage was designed to treat retinal degeneration. AGFB-ASA showed a prolonged release of 5-ASA. Upon pretreatment by intraperitoneal injection, the nanoglobular conjugate of 5-ASA produced a greater and more prolonged protective effect at a reduced dose against bright light-induced retinal degeneration in *Abca4*$^{-/-}$*Rdh8*$^{-/-}$ mice than free 5-ASA. The structure of nanoglobular drug conjugates can be further modified to optimize the release rate of a drug to achieve the best possible therapeutic efficacy. Nanosized nanoglobular 5-ASA conjugates with a degradable spacer show promise in protecting mouse retinas against light-induced retinal degeneration.

## MATERIALS AND METHODS

### Materials

Octa(3-aminopropyl)silsesquioxane hydrochloride (Octa Ammonium POSS-HCl) came from Hybrid Plastics (Hattiesburg, MS). $(Boc)_2$-L-lysine-OH and dioxane were purchased from Fisher Scientific (Pittsburg, PA). Pentafluorophenol (pfp-OH) was obtained from Oakwood Products, Inc. (Columbia, SC). 4-Formylbenzoic acid (FB) and diisopropyl ether were from Sigma-Aldrich (Louis, MO). Anhydrous *N*,*N*-diisopropylethylamine (DIPEA), dichloromethane (DCM), and *N*,*N*-dimethylformamide (DMF) were purchased from Alfa Aesar (Ward Hill, MA, USA). Trifluoroacetic acid (TFA) was obtained from ACROS Organics (Morris Plains, NJ, USA). All reagents were used without further purification.

### Synthesis of $(Boc)_2$-*L*-lysine-pfp

$(Boc)_2$-*L*-lysine-OH (11.3 g, 32.6 mmol), pfp-OH (6.00 g, 32.6 mmol), and *N*,*N*′-dicyclohexylcarbodiimide (DCC, 6.7 g, 33 mmol) were dissolved in 200 mL dioxane and the reaction mixture was stirred at room temperature overnight. After dioxane was removed under vacuum evaporation, the crude product was purified by crystallization twice in diisopropyl ether. The yield of $(Boc)_2$-*L*-lysine-pfp was 11.0 g, 66.0 %. MALDI-TOF (*m/z*, $[M + H]^+$): 512.47 (calculated), 512.10 (observed).

### Synthesis of (*L*-lysine)$_8$-OAS ($G_1$)

Octa(3-aminopropyl)silsesquioxane hydrochloride (OSA•8HCl, 1.2 g, 1.0 mmol), $(Boc)_2$-*L*-lysine-pfp (12.3 g, 24 mmol, 3 equivalents of amino groups), and diisopropylethylamine (DIPEA, 2.1 mL, 12 mmol, 1.5 equivalents of free amino groups) were dissolved in 25 mL DMF. The reaction mixture was stirred at room temperature for 24 h under $N_2$. The product then was precipitated by addition of ice-cold anhydrous diethyl ether. The dried precipitate of $[(t\text{-BOC})_2\text{-}L\text{-lysine}]_8$-OAS was dissolved in 30 mL TFA/DCM (1:1) and stirred at room temperature for 4 h to remove t-BOC groups. The resulting solution was concentrated under vacuum to a viscous oil. The residue was treated with ice-cold anhydrous diethyl ether to provide a white solid product. The yield of $(L\text{-lysine})_8$-OAS trifluoroacetate was 2.94 g (78.8 %). MALDI-TOF (*m/z*, $[M + H]^+$): 1907.20 (calculated for $C_{72}H_{160}N_{24}O_{20}Si_8$), 1907.04 (observed).

### Synthesis of (*L*-lysine)$_{16}$-(*L*-lysine)$_8$-OAS ($G_2$)

($L$-Lysine)$_8$-OAS ($G_1$) trifluoroacetate (2.5 g, 0.67 mmol), (Boc)$_2$-*L*-lysine-pfp (16.5 g, 32.2 mmol), and diisopropylethylamine (DIPEA, 2.8 ml, 16.1 mmol) were dissolved in 35 mL DMF. The reaction then was carried out as described for the synthesis of ($L$-lysine)$_8$-OAS. White ($L$-lysine)$_{16}$-($L$-lysine)$_8$-OAS ($G_2$) trifluoroacetate was obtained at a yield of 4.95 g, 98.0 %. MALDI-TOF (*m*/*z*, [M+ H]$^+$): 3956.63 (calculated for $C_{168}H_{352}N_{56}O_{36}Si_8$); 3956.84 (observed).

### Synthesis of $G_2$-FB

$G_2$ nanoglobule, ($L$-lysine)$_{16}$-($L$-lysine)$_8$-octa(3-aminopropyl) silsesquioxane (OAS) trifluoroacetate (2.0 g, 0.26 mmol) and DIPEA (2.2 ml, 13 mmol) were dissolved in 30 ml DMF. 4-Formylbenzoic pentafluorophenol activated ester solution (1.32 mmol, 5 equivalents to G2) in 60 ml DMF was slowly dripped into the G2 solution and the mixture was allowed to react in an ice-bath for 6 h. The filtered solution then was dripped into ice-cold ethyl ether, after which precipitates were collected and dried under vacuum to give compound 1 ($G_2$-FB). The yield of $G_2$-FB was 1.12 g, 92.1 %. MALDI-TOF (*m*/*z*, [M + Na]$^+$): 4639.24 (obsd.), 4640.21 (calculated from $G_2$ with 5 formylbenzoic acid groups).

### Acetylation of G2-FB to block free amine groups on $G_2$ (AGFB)

G2-FB (0.724 g, 0.156 mmol) was dissolved in 60 mL distilled water. Acetic anhydride (4.7 mL, 10 times the equivalent of free amino groups) was dripped in and the pH was maintained at 8.0 with triethylamine. The reaction was kept in an ice-bath for 4 h. Then the reaction solution was dialyzed with a membrane with molecular weight cutoff of 0.5–1.0 kDa overnight, and lyophilized to obtain compound AGFB. The yield of AGFB was 0.52 g, 59.9 %. MALDI-TOF (*m*/*z*, [M + Na]$^+$): 5773.71 (observed.), 5774.29 (calculated. from acetylated $G_2$ with 5 formylbenzoic acid groups).

### Synthesis of AGFB-ASA

AGFB (0.51 g, 0.088 mmol) was dissolved in 10 mL methanol. 5-ASA (0.15 g, 0.98 mmol, 2 times the equivalent of aldehyde groups) and a drop of acetic acid were added. The reaction was kept at room temperature overnight. Then the filtered solution was dropped into 100 mL of cold ethyl ether, precipitates were collected by centrifugation and re-dissolved in methanol. The crude product was purified by running it through a Sephadex G-15 column to remove free 5-ASA, the first yellow-brownish eluate was collected and dried under vacuum to give the final product compound AGFB-ASA. The yield of AGFB-ASA was 0.24 g, 42.4 %. MALDI-TOF (*m*/*z*, [M + Na]$^+$): 6020.91 (observed), 6428.80 (calculated), from acetylated $G_2$ conjugated with 5 drug molecules, ($C_{297}H_{451}N_{61}O_{83}Si_8$). $^1$H-NMR (300 MHz, $CD_3OD$, ppm): 8.63 (br, 5H, –CHN–), 8.07 and 7.93 (dm, 35H, –CH on benzene ring), 4.40– 4.21 (dm, 24H, –CH), 3.50–2.80 (br 16H, –$(CH_2)_3CH_2$; 16H, –$Si(CH_2)_2CH_2$; 32H, –$(CH_2)_3CH_2NH_2$), 1.76 (d, 81H, –$CH_3O$), 1.70–1.25 (br m, 32H, –$CHCH_2$; 16H, –$CHCH_2$; 32H, –$(CH_2)_2CH_2CH_2$; 16H, –$(CH_2)_2CH_2CH_2$; 32H, –$CH_2CH_2(CH_2)_2$, 16H, –$CH_2CH_2(CH_2)_2$; 16H, –$SiCH_2CH_2$), 0.63 (br, 16H, –$SiCH_2$).

### Synthesis of FB-ASA

4-Formylbenzoic acid (FB) (0.45 g, 3.0 mmol) and 5-ASA (0.15 g, 1.0 mmol) were added to 15 mL methanol. Acetic acid (4 SL) was then added to the reaction mixture which turned yellow after 10 minutes and was stirred at room temperature for 24 h. Precipitates were collected by centrifugation, washed with methanol 3 times, and dried under vacuum to provide the final product FB-ASA. The yield of FB-ASA was 240 mg, 84.2 %. MALDI-TOF (*m/z*, $[M + H]^+$): 285.25 (calculated for $C_{15}H_{11}NO_5$), 285.60 (observed). $^1$H-NMR (400 MHz, $(CD_3)_2SO$, ppm): 8.78 (s, 1H, –CHN–), 8.03 (d, 4H, –CH), 7.76 (d, 1H, –CH), 7.61 (dd, 1H, –CH), 7.03 (d, 1H, –CH).

### 5-ASA release experiments

Release of 5-ASA from the G2 conjugate by hydrolysis of the Schiff base was evaluated by using UV spectroscopy. Release of 5-ASA from 0.01 mM AGFB-ASA was measured in 0.05 M phosphate buffers at pH 7.4. Release of 5-ASA from 0.05 mM FB-ASA in pH 7.4 PBS was also tested as a control. Dendrimer conjugate solution or FB-ASA solution was incubated at 37 °C and samples were taken at selected time intervals up to 24 h. Immediately after sampling at each time point, samples were scanned from 200 nm to 450 nm with a SpectraMax M5 spectrometer (Molecular Devices, Sunnyvale, CA). Released drug from conjugates AGFB-ASA and FB-ASA in 0.05 M phosphate buffer, pH 7.4, after 1h was analyzed by HPLC (HPLC conditions: analytical C18 reverse column (250 mm × 4.6 mm, i.d., 5 Sm particle size) eluted with a mobile phase of $H_2O$: MeOH (80 : 20, *v/v*) with 0.05% trifluoroacetic acid, flow rate of 1.0 mL/min and UV detector set at 303 nm)

### Animal studies

With 4–5 animals used for each treatment group, 4-week-old *Abca4*$^{-/-}$*Rdh8*$^{-/-}$ mice[4] were kept in the dark for 48 h before each experiment. Then free 5-ASA (0.5 mg and 1.0 mg per mouse) or conjugate AGFB-ASA (4.3 mg and 8.6 mg per mouse, equivalent 0.5 and 1.0 mg free 5-ASA per mouse) was intraperitoneally injected 6 h before light exposure at 10,000 lux for 30 min. Mice then were kept in the dark for 7 days, after which final retinal evaluations were performed. Mice were anesthetized by intraperitoneal injection of a cocktail (20 μL $g^{-1}$ body weight) containing ketamine (6 mg $mL^{-1}$) and xylazine (0.44 mg $mL^{-1}$) in 10 mM sodium phosphate, pH 7.2, and 100 mM NaCl. Pupils were dilated with 0.01% tropicamide. Electroretinograms (ERGs) were recorded as previously reported[36]. All experimental procedures were performed under a safety light. A contact lens electrode was placed on the eye, and a reference electrode and ground electrode were placed underneath the skin between the two ears and in the tail, respectively. ERGs were recorded with the universal electrophysiologic system UTAS E-3000 (LKC Technologies, Inc., Gaithersburg, MD). The light intensity calibrated by the manufacturer was computer-controlled. Mice were placed in a Ganzfeld dome, and scotopic responses to flash stimuli were obtained from both eyes simultaneously. Retinas of mice were then imaged *in vivo* with ultra-high resolution spectral-domain OCT (SD-OCT; Bioptigen, Irvine, CA) 24 h after the ERG test. Dark-adapted mice were anesthetized according to the same protocol used for ERG. Five pictures acquired in the Bscan mode were used to construct each final averaged SD-OCT image.

Quantitative morphometric obtained from ONL thickness was measured from OCT images along the horizontal meridian from the nasal to temporal retina.

## Acknowledgments

The authors thank Dr. Erlei Jin for valuable advice about the involved chemistry. This work was supported in part by funding from the National Eye Institute of the National Institutes of Health (grants R24EY021126. K.P. is John H. Hord Professor of Pharmacology.)

## References

1. Maeda T, Golczak M, Maeda A. Retinal Photodamage Mediated by All-*Trans*-Retinal. Photochem Photobiol. 2012; 88:1309–1319. [PubMed: 22428905]
2. Kiser PD, Golczak M, Maeda A, Palczewski K. Key Enzymes of the Retinoid (Visual) Cycle in Vertebrate Retina. Biochim Biophys Acta. 2012; 1821:137–151. [PubMed: 21447403]
3. Palczewski K. Retinoids for Treatment of Retinal Diseases. Trends Pharmacol Sci. 2010; 31:284–295. [PubMed: 20435355]
4. Maeda A, Maeda T, Golczak M, Palczewski K. Retinopathy in Mice Induced by Disrupted All-*Trans*-Retinal Clearance. J Biol Chem. 2008; 283:26684–26693. [PubMed: 18658157]
5. Maeda A, Golczak M, Chen Y, Okano K, Kohno H, Shiose S, Ishikawa K, Harte W, Palczewska G, Maeda T, et al. Primary Amines Protect Against Retinal Degeneration in Mouse Models of Retinopathies. Nat Chem Biol. 2012; 8:170–178. [PubMed: 22198730]
6. Klotz U, Maier KE. Pharmacology and Pharmacokinetics of 5-Aminosalicylic Acid. Dig Dis Sci. 1987; 32:S46–S50.
7. Gaudana R, Ananthula HK, Parenky A, Mitra AK. Ocular Drug Delivery. AAPS J. 2010; 12:348–360. [PubMed: 20437123]
8. Geroski DH, Edelhauser HF. Drug Delivery for Posterior Segment Eye Disease. Invest Ophthalmol Vis Sci. 2000; 41:961–964. [PubMed: 10752928]
9. Del Amo EM, Urtti A. Current and Future Ophthalmic Drug Delivery Systems. A Shift to the Posterior Segment. Drug Discov Today. 2008; 13:135–143. [PubMed: 18275911]
10. Eljarrat-Binstock E, Pe'er J, Domb AJ. New Techniques for Drug Delivery to the Posterior Eye Segment. Pharm Res. 2010; 27:530–543. [PubMed: 20155388]
11. Chastain, JE. General Considerations in Ocular Drug Delivery. In: Mitra, AK., editor. Ophthalmic Drug Delivery Systems. Marcel Dekker, Inc; New York: 2003. p. 59-107.
12. Edelhauser HF, Rowe-Rendleman CL, Robinson MR, Dawson DG, Chader GJ, Grossniklaus HE, Rittenhouse KD, Wilson CG, Weber DA, Kuppermann BD, et al. Ophthalmic Drug Delivery Systems for the Treatment of Retinal Diseases: Basic Research to Clinical Applications. Invest Ophthalmol Vis Sci. 2010; 51:5403–5420. [PubMed: 20980702]
13. Babu VR, Mallikarjun V, Nikhat SR, Srikanth G. Dendrimers: A New Carrier System for Drug Delivery. Int J Pharm Appl Sci. 2010; 1:1–10.
14. Vandamme TF. Microemulsions as Ocular Drug Delivery Systems: Recent Developments and Future Challenges. Prog Retin Eye Res. 2002; 21:15–34. [PubMed: 11906809]
15. Kaur IP, Garg A, Singla AK, Aggarwal D. Vesicular Systems in Ocular Drug Delivery: An Overview. Int J Pharm. 2004; 269:1–14. [PubMed: 14698571]
16. Barbu E, Verestiuc L, Iancu M, Jatariu A, Lungu A, Tsibouklis J. Hybrid Polymeric Hydrogels for Ocular Drug Delivery: Nanoparticulate Systems from Copolymers of Acrylic Acid-Functionalized Chitosan and *N*-Isopropylacrylamide or 2-Hydroxyethyl Methacrylate. Nanotechnology. 2009; 20:225108, 10. [PubMed: 19433871]
17. Hacker MC, Haesslein A, Ueda H, Foster WJ, Garcia CA, Ammon DM, Borazjani RN, Kunzler JF, Salamone JC, Mikos AG. Biodegradable Fumarate-Based Drug-Delivery Systems for Ophthalmic Applications. J Biomed Mater Res A. 2009; 88:976–989. [PubMed: 18384171]
18. Jiang J, Moore JS, Edelhauser HF, Prausnitz MR. Intrascleral Drug Delivery to the Eye Using Hollow Microneedles. PharmRes. 2009; 26:395–403.

19. Kim YC, Park JH, Prausnitz MR. Microneedles for Drug and Vaccine Delivery. Adv Drug Deliv Rev. 2012; 64:1547–1568. [PubMed: 22575858]
20. Shirasaki Y. Molecular Design for Enhancement of Ocular Penetration. J Pharm Sci. 2008; 97:2462–2496. [PubMed: 17918725]
21. Wadhwa S, Paliwal R, Paliwal SR, Vyas SP. Nanocarriers in Ocular Drug Delivery: An Update Review. Curr Pharm Des. 2009; 15:2724–2750. [PubMed: 19689343]
22. Kuno N, Fujii S. Recent Advances in Ocular Drug Delivery Systems. Polymers. 2011; 3:193–221.
23. Cheng YY, Xu ZH, Ma ML, Xu TW. Dendrimers as Drug Carriers: Applications in Different Routes of Drug Administration. J Pharm Sci. 2008; 97:123–143. [PubMed: 17721949]
24. Medina SH, El-Sayed MEH. Dendrimers as Carriers for Delivery of Chemotherapeutic Agents. Chem Rev. 2009; 109:3141–3157. [PubMed: 19534493]
25. Durairaj C, Kadam RS, Chandler JW, Hutcherson SL, Kompella UB. Nanosized Dendritic Polyguanidilyated Translocators for Enhanced Solubility, Permeability, and Delivery of Gatifloxacin. Invest Ophthalmol Vis Sci. 2010; 51:5804–5816. [PubMed: 20484584]
26. Vandamme TF, Brobeck L. Poly(amidoamine) Dendrimers as Ophthalmic Vehicles for Ocular Delivery of Pilocarpine Nitrate and Tropicamide. J Control Release. 2005; 102:23–38. [PubMed: 15653131]
27. Kambhampati SP, Kannan RM. Dendrimer Nanoparticles for Ocular Drug Delivery. J Ocul Pharmacol Ther. 2013; 29:151–165. [PubMed: 23410062]
28. Yang H, Tyagi P, Kadam RS, Holden CA, Kompella UB. Hybrid Dendrimer Hydrogel/PLGA Nanoparticle Platform Sustains Drug Delivery for One Week and Antiglaucoma Effects for Four Days Following One-Time Topical Administration. ACS Nano. 2012; 6:7595–7606. [PubMed: 22876910]
29. Iezzi R, Guru BR, Glybina IV, Mishra MK, Kennedy A, Kannan RM. Dendrimer-Based Targeted Intravitreal Therapy for Sustained Attenuation of Neuroinflammation in Retinal Degeneration. Biomaterials. 2012; 33:979–988. [PubMed: 22048009]
30. Holden CA, Tyagi P, Thakur A, Kadam R, Jadhav G, Kompella UB, Yang H. Polyamidoamine Dendrimer Hydrogel for Enhanced Delivery of Antiglaucoma Drugs. Nanomedicine. 2012; 8:776–783. [PubMed: 21930109]
31. Kaneshiro TL, Wang X, Lu ZR. Synthesis, Characterization, and Gene Delivery of Poly-L-lySine Octa(3-aminopropyl)silsesquioxane Dendrimers: Nanoglobular Drug Carriers with Precisely Defined Molecular Architectures. Mol Pharm. 2007; 4:759–768. [PubMed: 17705440]
32. Kaneshiro TL, Jeong EK, Morrell G, Parker DL, Lu ZR. Synthesis and Evaluation of Globular Gd-DOTA-Monoamide Conjugates with Precisely Controlled Nanosizes for Magnetic Resonance Angiography. Biomacromolecules. 2008; 9:2742–2748. [PubMed: 18771313]
33. Kratz F, Beyer U, Schutte MT. Drug-polymer Conjugates Containing Acid-Cleavable Bonds. Crit Rev Ther Drug Carrier Syst. 1999; 16:245–288. [PubMed: 10706520]
34. Saito H, Hoffman AS, Ogawa HI. Delivery of Doxorubicin from Biodegradable PEG Hydrogels Having Schiff base Linkages. J Bioactive Compat Polym. 2007; 22:589–601.
35. Tan MQ, Wu XM, Jeong E-K, Chen QJ, Lu ZR. Peptide-Targeted Nanoglobular Gd-DOTA Monoamide Conjugates for Magnetic Resonance Cancer Molecular Imaging. Biomacromolecules. 2010; 11:754–761. [PubMed: 20131758]
36. Maeda A, Maeda T, Golczak M, Imanishi Y, Leahy P, Kubota R, Palczewski K. Effects of Potent Inhibitors of the Retinoid Cycle on Visual Function and Photoreceptor Protection from Light Damage in Mice. Mol Pharmacol. 2006; 70:1220–1229. [PubMed: 16837623]

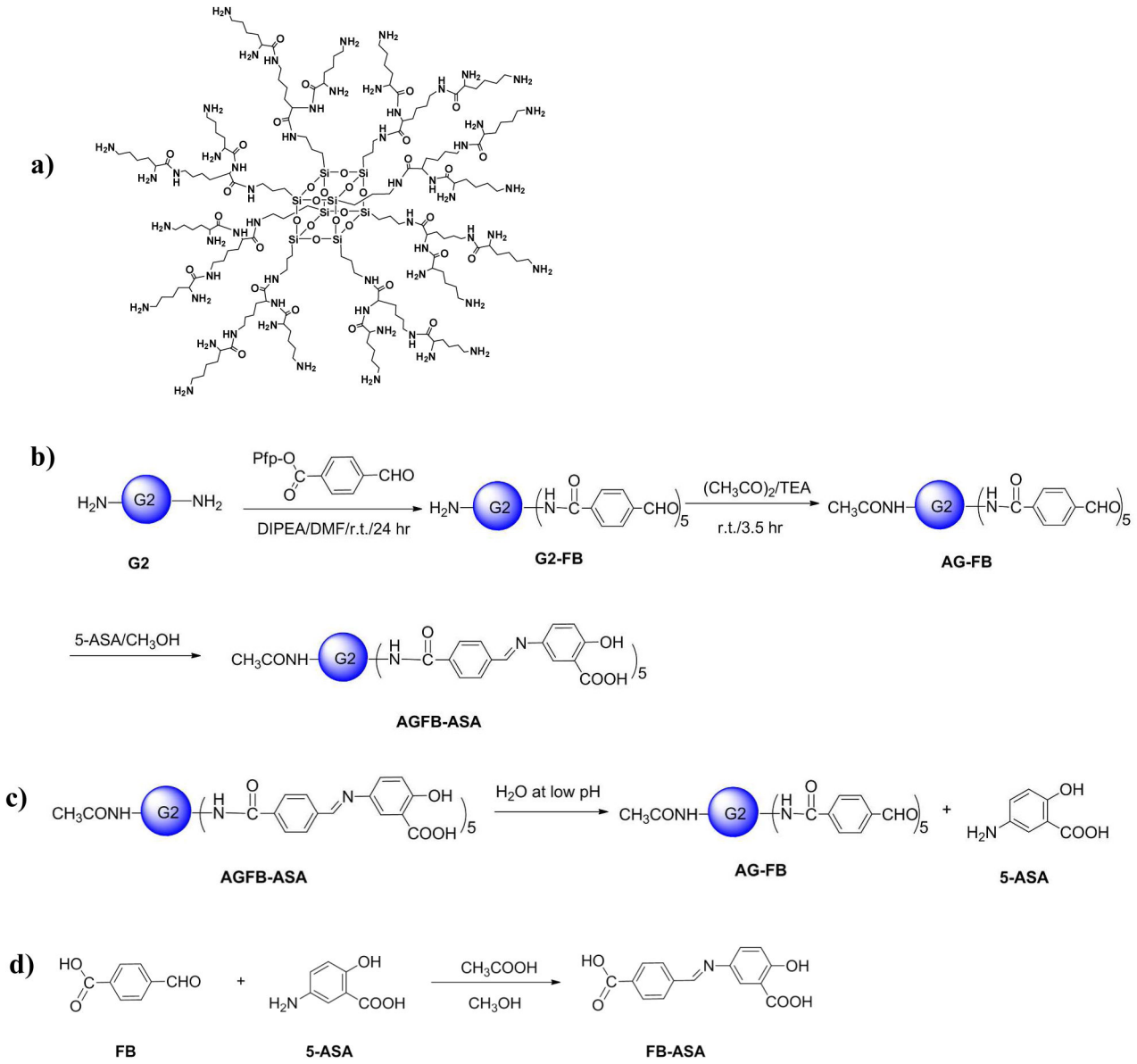


**Fig. 1.**

The AGFB-ASA conjugate: structure, synthesis and release of 5-ASA. (a) Structure of the nanoglobular dendrimer $G_2$; (b) scheme of AGFB-ASA conjugate synthesis; (c) 5-ASA release from the conjugate; (d) scheme of FB-ASA conjugate synthesis.

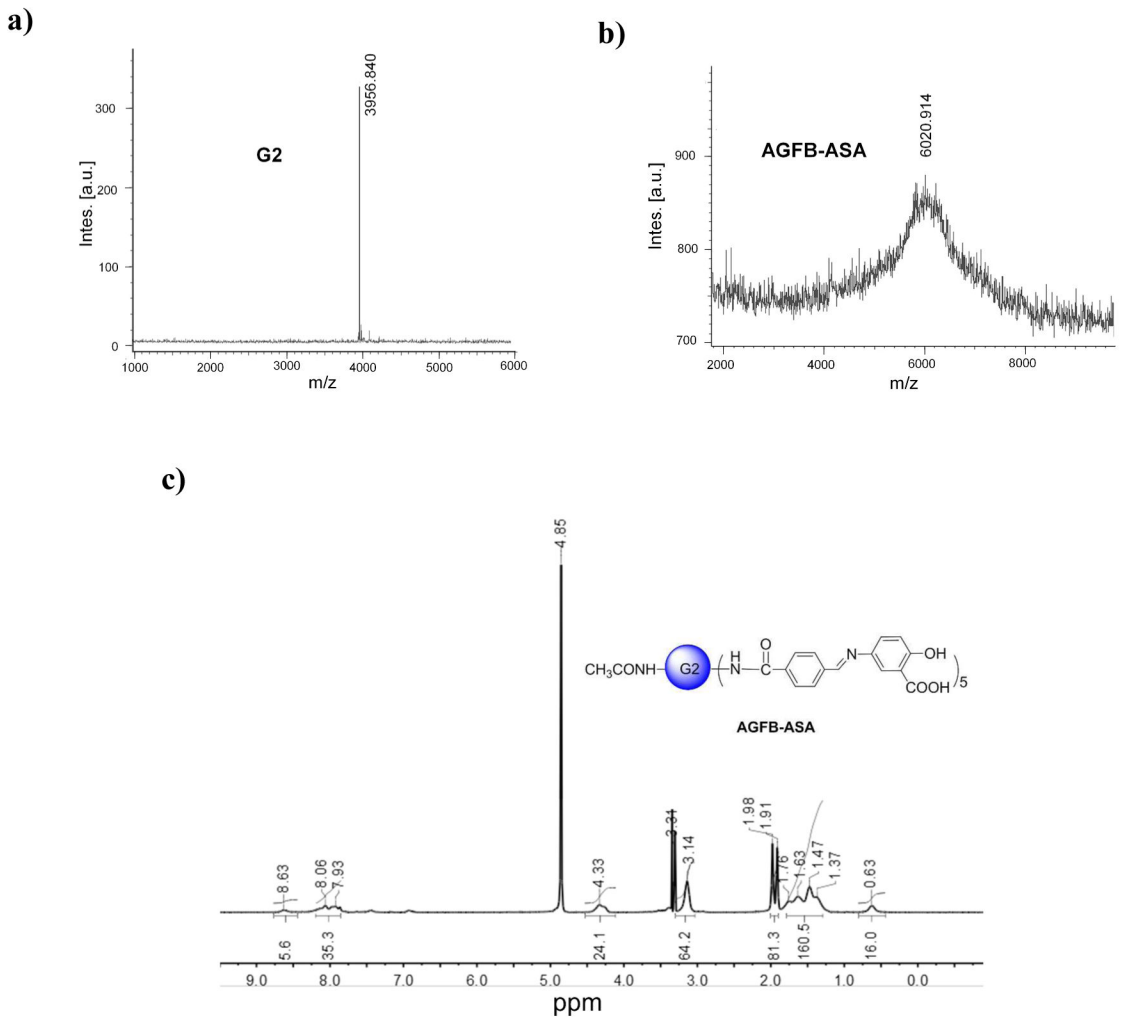


**Fig. 2.**

Characterization of the conjugate. (a) MALDI-TOF spectrum of G2; (b) MALDI-TOF spectrum of the final conjugate, AGFB-ASA; (c) $^{1}$H-NMR spectrum of the AGFB-ASA conjugate.

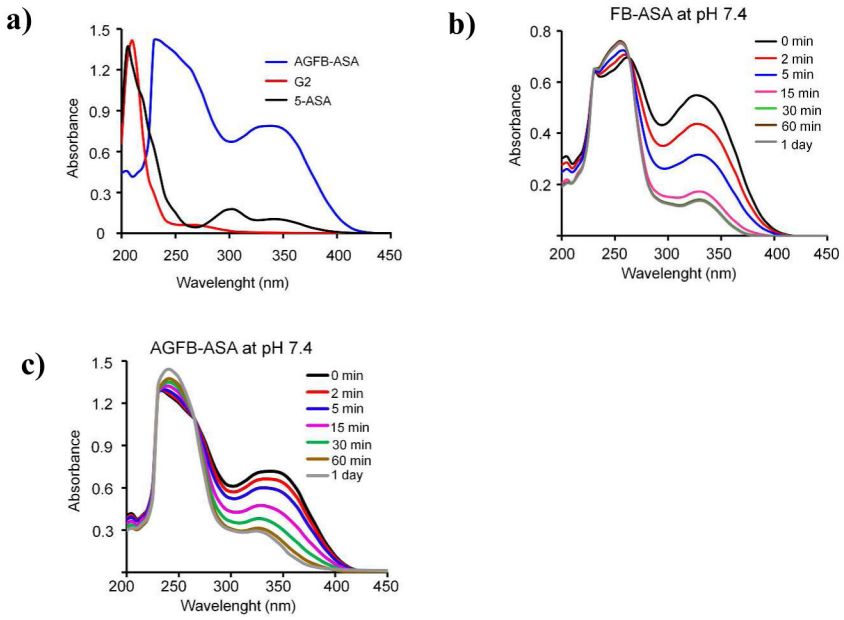


**Fig. 3.**

Dynamic UV spectra showing drug release kinetics from the Schiff base conjugate. (**a**) UV spectra for AGFB-ASA, G2 and 5-ASA in PBS at pH 7.4; (**b**) FB-ASA in PBS at pH 7.4; (**c**) AGFB-ASA in PBS at pH 7.4.

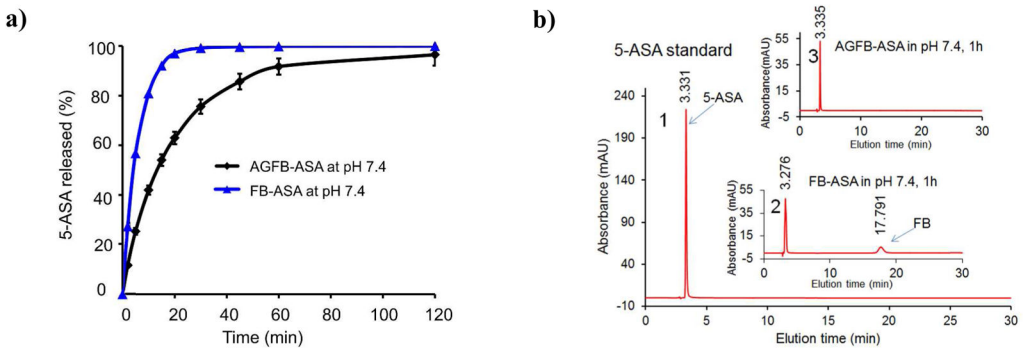


**Fig. 4.**

*In vitro* drug release kinetics for the conjugates. (a) Release kinetic profiles of 5-ASA from AGFB-ASA in PBS at pH 7.4, and from FB-ASA in PBS at pH 7.4 assayed by UV spectroscopy; (b) HPLC analyses of the released products: (**1**) 5-ASA standard, (**2**) FB-ASA in PBS at pH 7.4 at 1 h, (**3**) AGFB-ASA in PBS at pH 7.4 PBS. HPLC conditions: analytical C18 reverse column (250 mm × 4.6 mm, i.d., 5 μm particle size) with a mobile phase of $H_2O$ : MeOH (80 : 20, *v*/*v*) with 0.05% trifluoroacetic acid, flow rate of 1.0 mL/min and UV detector set at 303 nm.

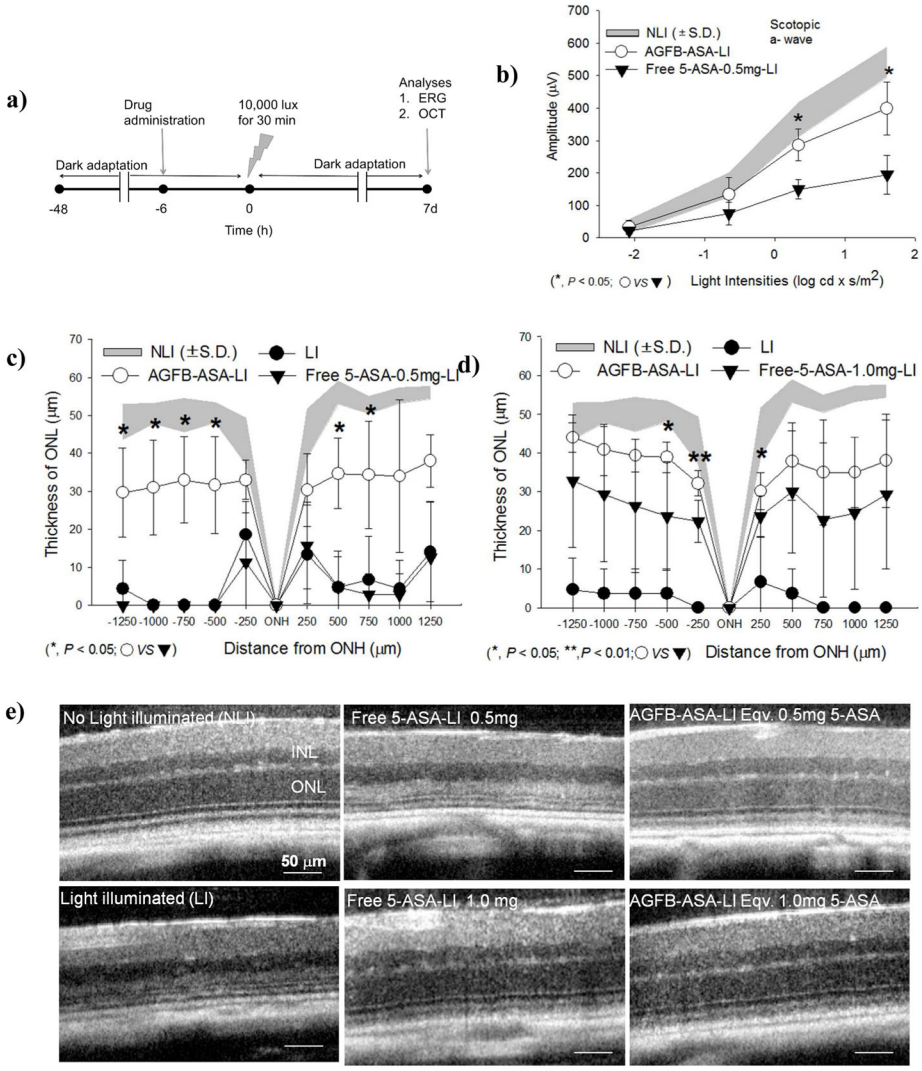


**Fig. 5.**

Protective effects of AGFB-ASA and free 5-ASA pretreatment on the development of acute light-induced retinal degeneration in *Abca4*$^{-/-}$*Rdh8*$^{-/-}$ mice (NLI = No light illumination; LI = Light illuminated). (**a**) Schematic representation of the experimental design. After 4-week-old *Abca4*$^{-/-}$*Rdh8*$^{-/-}$ mice were kept in the dark for 48 h, either free 5-ASA or conjugate AGFB-ASA were intraperitoneally injected at a dose equivalent to 0.5 mg or 1.0 mg 5-ASA per mouse 6 h before light exposure at 10,000 lux for 30 min. Mice were then kept in the dark for 7 days, after which final retinal evaluations were performed. (**b**) ERG responses of pretreated *Abca4*$^{-/-}$*Rdh8*$^{-/-}$ mice at 4 weeks age with free 5-ASA or conjugate AGFB-ASA at a dose of 0.5 mg 5-ASA per mouse prior to light illumination and evaluated 7 day later. ERG responses were recorded under scotopic conditions. Error bars indicate S.D. of the means (n = 3). ONL thicknesses were measured from OCT images obtained along the horizontal meridian from the nasal to temporal retina: (**c**) 0.5 mg 5-ASA per mouse (**d**) 1.0 mg 5-ASA per mouse. Statistical analyses were performed by the two-way analysis of variance (Student's T-test). Error bars indicate S.D. of the means (n = 4 – 5). (**e**) OCT

images indicate representative morphology of *Abca4*$^{-/-}$*Rdh8*$^{-/-}$ mouse retinas. Scale bar indicates 50 μm in the OCT image.